

9 Density Matrix Renormalization

Karen Hallberg

Centro Atómico Bariloche and Instituto Balseiro
San Carlos de Bariloche, Argentina

Contents

1	Introduction	2
2	Calculating ground states with the DMRG	2
2.1	Definitions and method	3
2.2	Quantum information analysis	5
2.3	Standard algorithm	5
3	Calculating dynamical quantities with the DMRG	7
3.1	Lanczos dynamics	8
3.2	Correction vector dynamics	8
4	Using the DMRG as the impurity solver for dynamical mean-field theory	9
4.1	Implementation for multi-site and multi-orbital problems	10
5	Conclusions	14

1 Introduction

The density matrix renormalization group (DMRG) has evolved to become one of the most reliable and versatile numerical methods in modern computational physics. It allows for a very precise calculation of ground states and excitations of strongly correlated fermionic and bosonic systems. After its original inception by S. White in 1992 [1, 2], when it was developed to solve problems in low-dimensional quantum condensed matter, it has been extended to other fields as well, and it is now being successfully used in quantum chemistry, statistical mechanics, quantum information theory, nuclear and high-energy physics. It has been applied to a great variety of systems and problems such as spin chains and ladders, fermionic and bosonic systems, disordered models, impurities, molecules, nanoscopic systems as well as 2D electrons in high magnetic fields. And extensions to the method include two dimensional (2D) classical systems, stochastic models, phonons, quantum chemistry, field theory, finite temperature and the calculation of dynamical and time-dependent properties. Some calculations have also been performed in 2D quantum systems.

In this chapter we will introduce the basic formulation of the DMRG. We will also delve on the extension of this method to calculate dynamical behavior and show how this was implemented to enhance the performance of one of the most reliable methods to solve correlated matter, dynamical mean-field theory (DMFT).

Among the several reviews, I recommend the basic textbook [3] and reviews such as [4–6]. For newcomers to the field, it is advisable to visit the ALPS code library, containing state-of-the-art methods for solving interacting quantum systems [8] and the website containing updated information on the DMRG and publications [9].

The development DMRG has paved the way to the rich and promising world of tensor networks (see the chapter by Miles Stoudenmire in this book). A comprehensive set of lectures is given in [10]. There is a very useful library for tensor network calculations in [11].

2 Calculating ground states with the DMRG

When working with quantum systems one encounters the exponential problem, i.e., the total number of states of the systems grows exponentially with system size. In non-interacting or weakly interacting systems, one can make approximations and solve for one particle, assuming that the result will depend very weakly on the number of particles. For more strongly interacting systems, however, this is not possible and a many-body calculation is necessary. Let's consider, for example, a quantum spin chain with spins $S = 1/2$ in each of the N sites of the chain. The total Hilbert space grows exponentially as 2^N , and this is the size of the operators, in particular of the Hamiltonian, to be diagonalized to solve the system. This means that the problem becomes intractable very quickly (currently, using exact diagonalization one cannot solve for more than around $N = 30$ sites).

The first successful renormalization of a correlated systems was done by K. Wilson when he developed the Numerical Renormalization Group for the single impurity Anderson model [12].

However, later attempts to apply real space renormalization techniques to quantum correlated models led to poor results, as for example, the attempts to solve the 1D Hubbard model [13], for which the system was separated into several blocks and only the lowest-lying energy levels were kept for the new iterations. White and Noack [14] realized that one of the main problems with these real space renormalizations was the separation of the basic blocks into separate entities, so they tried solving the problem by including varying boundary conditions between them. This basic idea led White to think about using the reduced density matrix defined in part of the system as a new criterion to choose the relevant states. As we will show below, this idea solved the block boundary problem and provided a straightforward way to discard non relevant states. This led to the development of the DMRG, which proved to be one of the most accurate numerical methods to solve interacting quantum problems.

The DMRG is based on a systematic truncation of the Hilbert space by keeping the most probable states describing one or several wave functions. These wave functions will be called the target states since they will be the ones we are aiming to describe in an accurate way (for example, they could be the ground state, of some excited states). The truncations are done by calculating the reduced density matrix in part of the system and keeping only its eigenvectors with the highest eigenvalues. As we will show below, the eigenvalue is the weight of its corresponding eigenvector in the target wave function. So from here it is clear that this is a good criterion to trim the Hilbert space.

We will start with the standard DMRG as it was originally developed by S. White [1,2]. Since then there have been other ways of implementing the same basic idea of using the information provided by the density matrix to reduce the Hilbert space. These methods include the matrix product state (MPS) representation [15]

2.1 Definitions and method

Before writing the algorithm explicitly we need to define some basic concepts. The method is based on the partitioning the whole lattice into two parts, S being the system and E the environment. This way, states $|i\rangle$ are part of S and states $|j\rangle$ form E . Any state of the whole lattice $|\psi\rangle$ can be written as

$$|\psi\rangle = \sum_{i,j} \psi_{ij} |i\rangle |j\rangle.$$

Given this bipartition, any operator acting only on the system S can be calculated as

$$\langle\psi|O^S|\psi\rangle = \sum_{ij,i'j'} \psi_{i'j'}^* \psi_{ij} \langle i'j'|O^S|ij\rangle = \sum_{ij,i'} \psi_{i'j}^* \psi_{ij} \langle i'|O^S|i\rangle = \sum_{ii'} O_{ii'}^S \underbrace{\sum_j \psi_{ij} \psi_{i'j}^*}_{\rho_{ii'}^S} = \text{Tr} \rho^S O^S.$$

Here we have straightforwardly defined the reduced density matrix $\rho^S = \text{Tr}_E |\psi\rangle\langle\psi|$ which is defined in S and has the following properties:

- it is Hermitian: $\rho^{S\dagger} = \rho^S$
- $\text{Tr} \rho^S = \sum_{\alpha} w_{\alpha} = 1$
- it is positive-semidefinite (so all eigenvalues are $w_{\alpha} \geq 0$)

In the diagonal basis $\rho^S = \sum_{\alpha} w_{\alpha} |w_{\alpha}\rangle\langle w_{\alpha}|$, so the mean value of the operator on S is

$$\langle \psi | O^S | \psi \rangle = \text{Tr}_S \rho^S O^S = \sum_{\alpha} w_{\alpha} \langle w_{\alpha} | O^S | w_{\alpha} \rangle. \quad (1)$$

When more than one target state is used, the density matrix is defined as

$$\rho_{ii'}^S = \sum_l p_l \sum_j \psi_{l,ij} \psi_{l,i'j}, \quad (2)$$

where p_l defines the probability of finding the system in the target state $|\psi_l\rangle$ (not necessarily an eigenstate of the Hamiltonian).

It can be easily shown [2] that the density matrix eigenvalues w_{α} represent the probability of the state $|\psi\rangle$ being in substate $|w_{\alpha}\rangle$. The density matrix leads directly to the optimal states in the system as we demonstrate below.

We define again

$$|\psi\rangle = \sum_{i,j=1}^{M,M'} \psi_{ij} |i\rangle |j\rangle \quad (3)$$

as a state of the $S+E$, having real coefficients for simplicity. Our aim is to obtain a variational wave function $|\hat{\psi}\rangle$ defined in an optimally reduced space, generated by the m vectors of S , $|\alpha\rangle = \sum_{i=1}^m u_{\alpha i} |i\rangle$,

$$|\hat{\psi}\rangle = \sum_{\alpha=1}^m \sum_{j=1}^M a_{\alpha j} |\alpha\rangle |j\rangle \quad (4)$$

such that the difference with the original wave function is minimal with respect to $a_{\alpha j}$

$$||\psi\rangle - |\hat{\psi}\rangle|^2 = 1 - 2 \sum_{\alpha ij} \psi_{ij} a_{\alpha j} u_{\alpha i} + \sum_{\alpha j} a_{\alpha j}^2. \quad (5)$$

This condition leads to

$$\sum_i \psi_{ij} u_{\alpha i} = a_{\alpha j}. \quad (6)$$

Using the definition of the reduced density matrix for S

$$\rho_{ii'}^S = \sum_j \rho_{ij,i'j} = \sum_j \langle j | \langle i | \psi \rangle \langle \psi | i' \rangle | j \rangle = \sum_j \psi_{ij} \psi_{i'j}, \quad (7)$$

and placing (6) into Eq. (5) we obtain

$$1 - \sum_{\alpha ii'} u_{\alpha i} \rho_{ii'}^S u_{\alpha i'} = 1 - \sum_{\alpha=1}^m \omega_{\alpha}, \quad (8)$$

where $u_{\alpha i}$ is the operator that changes basis from $|i\rangle$ to $|\alpha\rangle$, and ω_{α} are the density-matrix eigenvalues. The above expression is minimum for the largest eigenvalues of the density matrix ρ^S , which are all positive or zero and the last term corresponds to the discarded error.

So, summarizing, the best approximation to $|\psi\rangle$ is done by considering the highest eigenvalued (most probable) eigenstates of ρ^S when trimming the basis states. This is the basic mechanism of the DMRG.

2.2 Quantum information analysis

It is useful to consider concepts from quantum information, such as the von Neumann entropy

$$S_{vN} = - \sum_{\alpha} w_{\alpha} \log w_{\alpha} = - \text{Tr} \rho^S \log \rho^S. \quad (9)$$

This quantum entropy gives a quantitative measure of the entanglement between S and E if the target state $|\psi\rangle$ is a pure state. The larger the entropy, the larger the entanglement. If, for example, ρ^S has only one eigenvalue $w_1 = 1$, then there is only one eigenvector in each block and $|\psi\rangle$ is a product state with no entanglement. If the w_{α} decrease rapidly, then it is sufficient to consider only the largest eigenvalues to have a reliable representation of the target state $|\psi\rangle$. The worst case scenario happens when there is no information about the state and all w_{α} have the same value so $S_{vN} = N$, the system size. S_{vN} is the number of qubits (sites with two degrees of freedom) one has to consider to describe the state, so one can estimate that the number of states m one should keep without losing crucial information is $m \sim 2^{S_{vN}}$. The DMRG works best for low quantum entangled systems (it is particularly exact for product states).

This analysis gives us a good insight into the DMRG performance in different systems and dimensions. By using geometric arguments in a $d+1$ -dimensional field theory including a $d-1$ -dimensional hypersurface dividing the system in two, $S+E$, it is shown that the entropy resides essentially at the surface and scales as the area of the hypersurface [16]

$$S_{vN}(L) \propto (L/\lambda)^{d-1}, \quad (10)$$

where λ is an ultraviolet cutoff and L the linear dimension. In one dimension, $d = 1$, a more detailed calculation for gap-less critical systems leads to a logarithmic scaling of the entropy, $S_{vN}(L) = c/3 \ln(L) + \lambda_1$, where c is the central charge of the underlying conformal field theory. A saturated entropy for non critical, gapped systems is obtained [17–19] when the system size exceeds the correlation length. In two dimensions $S_{vN} \sim L$, so one expects a poorer performance of the DMRG.

2.3 Standard algorithm

Now we are ready to introduce the main algorithm in the standard implementation. As said, the DMRG is based on a systematic truncation of the Hilbert space by keeping the most probable states describing a target wave function (e.g. the ground state, or excited states). For this, it is important to define the space in which the Hamiltonian operates (for example, real space, but a description in momentum, orthonormal orbitals or energy space is also feasible). The elements of this space (sites, momenta, orbitals, or energies) are ordered in a one-dimensional way and then it is partitioned into two, not necessarily equal, parts. From now on we will call them sites without loss of generality. In its classical formulation, one begins with a growing or “warm-up” phase starting with a small system, e.g., with N_0 sites, and then gradually increase its size to N_0+2, N_0+4, \dots until the desired length N is reached.

Based on Fig. 1 we define block $[B]$ as a finite chain with l sites having an associated Hilbert space with m states in which operators such as the block Hamiltonian H_B , connecting, and correlation operators are defined and expressed in matrix form. Except for the first iteration, the basis in this block is not explicitly known due to previous basis rotations and reductions which are non-unitary if there has been a reduction of states. An additional site with n states is defined as $[a]$. For a general iteration our system S is formed by blocks $[B]$ and $[a]$: $S = [B] \otimes [a]$. Equivalently, the environment is $E = [a'] \otimes [B']$ (see Fig. 1).

To illustrate the general iteration let us consider the one-dimensional spin $S = 1/2$ Heisenberg Hamiltonian

$$H = \sum_i \mathbf{S}_i \mathbf{S}_{i+1} = S_i^z S_{i+1}^z + \frac{1}{2} (S_i^+ S_{i+1}^- + S_i^- S_{i+1}^+). \quad (11)$$

The general iteration runs as follows:

- (i) Define the Hamiltonian $H_{BB'}$ for the whole system [20] $S+E = [Baa'B']$:

$$[H_{B_1 B_2}]_{ij;i'j'} = [H_{B_1}]_{ii'} \delta_{jj'} + [H_{B_2}]_{jj'} \delta_{ii'} + [S_a^z]_{ii'} [S_{a'}^z]_{jj'} + \frac{1}{2} [S_a^+]_{ii'} [S_{a'}^-]_{jj'} + \frac{1}{2} [S_a^-]_{ii'} [S_{a'}^+]_{jj'} \quad (12)$$

- (ii) Diagonalize $H_{BB'}$ to obtain the ground state $|\psi\rangle$ or other states (target states) using the Lanczos [21] or Davidson [22] algorithms.

- (iii) Calculate the density matrix

$$\rho_{ii'}^S = \sum_j \psi_{ij} \psi_{i'j} \quad (13)$$

on block $S=[Ba]$ defined by states i , tracing over the bath $E=[B'a']$ defined by states j .

- (iv) Diagonalize ρ^S and keep the m states with the largest eigenvalues. The truncation error is $1 - \sum_{\alpha=1}^m \omega_\alpha$, which should be kept small, typically much less than 10^{-6} .

- (v) Rotate and change basis of all operators in $[Ba]$ and simultaneously redefine $[Ba] \rightarrow [B]$: for example $H_B = O^\dagger H_{Ba} O$, where O is a rectangular matrix.

- (vi) A new block $[a]$ is added (one site in our case) and the iteration goes back to (i)

Once the desired length N is reached a higher accuracy can be obtained by sweeping to and fro a couple of iterations along the chain without changing N . The block sizes change with the internal variable l as $[Baa'B']$, $N = l+1+1+l'$ where l and $l' = N-l-2$ are the number of sites in B and B' respectively. The density matrix is used to project onto the growing block and stored operators from previous iterations are used for the shrinking block.

It saves time and memory to include symmetries in the DMRG algorithm. For example, for a spin model like the one mentioned above, the total spin z projection S_z is conserved, which is the sum of the spin projections of each constituting block. Total particle number is also a common symmetry that can be easily implemented. When the total quantum number can be

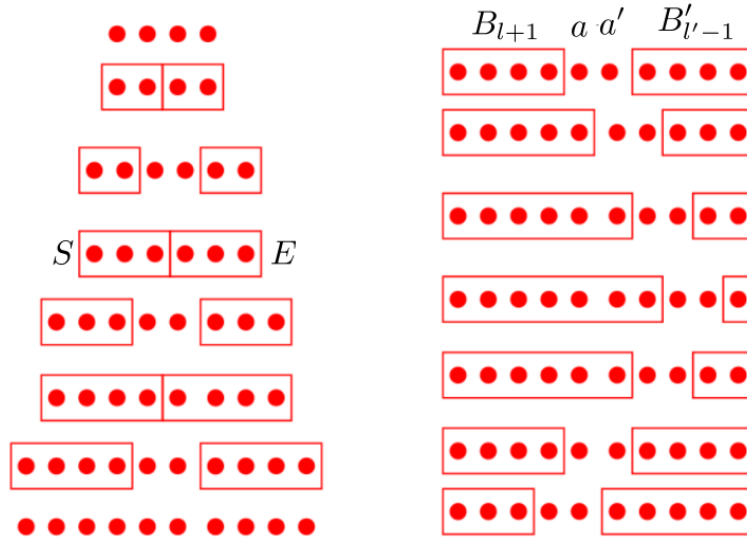


Fig. 1: Iterations of the classical DMRG. Left: warm up growth. Right: Finite-size sweeps. Here system S and environment E are also defined, as well as the blocks used in the iterations.

obtained as an addition of quantum numbers of each block of the system, the density matrix is block diagonal: if the global state $|\psi\rangle = \sum_{i,j} \psi_{ij} |i\rangle |j\rangle$ has N_p particles, $\psi_{ij} = \psi_{ij} \delta_{N_i+N_j, N_p}$, where N_i is the particle number of state $|i\rangle$, the reduced density matrix is

$$\rho_{ii'}^S = \sum_j \psi_{ij} \psi_{i'j}^* = \sum_j \psi_{ij} \psi_{i'j}^* \delta_{N_i+N_j, N_p} \delta_{N_{i'}+N_j, N_p} = \sum_j \psi_{ij} \psi_{i'j}^* \delta_{N_i N_{i'}} ,$$

which is block diagonal with a fixed particle number N_i . The eigenstates of ρ^S will then also have a defined particle number and this means that the renormalization maintains the particle number symmetry. Non abelian or non additive symmetries like $SU(2)$ or total spin are more difficult to implement, however possible in some cases.

3 Calculating dynamical quantities with the DMRG

The density matrix renormalization group can also be used to calculate dynamical properties (mainly at zero temperature) of low-dimensional systems, which are useful to interpret experimental results from, for example, nuclear magnetic resonance (NMR), neutron scattering, optical absorption and photoemission, among others.

The main current approaches for the calculation of spectral functions include the Lanczos method [23–26], the correction vector technique (CV) [24, 27, 28], Fourier transformation of time-dependent excitations [29–32] and Chebyshev polynomials [33, 34].

In this lecture we will focus on the two first ones: the Lanczos dynamics gives complete information of the whole excitation spectrum at the expense of less accuracy for large systems, specially at high energies, while the CV focuses on particular energy values and gives more precise information, being numerically much more expensive, unless the program is parallelized, so several energy values are calculated simultaneously.

We define the following dynamical correlation function at $T = 0$

$$C_A(t-t') = \langle \psi_0 | A^\dagger(t) A(t') | \psi_0 \rangle, \quad (14)$$

where A^\dagger is the Hermitian conjugate of the operator A (other operators are also feasible with slight changes in the formulation), $A(t)$ is the Heisenberg representation of A , and $|\psi_0\rangle$ is the ground state of the system. Its Fourier transform can be written in the Lehmann representation

$$C_A(\omega) = \sum_n |\langle \psi_n | A | \psi_0 \rangle|^2 \delta(\omega - (E_n - E_0)) = -\frac{1}{\pi} \lim_{\eta \rightarrow 0^+} \text{Im} G_A(\omega + i\eta + E_0), \quad (15)$$

where the sum is taken over all the eigenstates $|\psi_n\rangle$ of the Hamiltonian H with energy E_n , E_0 is the ground state energy, and the Green function is defined as

$$G_A(z) = \langle \psi_0 | A^\dagger (z - H)^{-1} A | \psi_0 \rangle, \quad (16)$$

where $z = w + i\eta$ and η is a small shift towards imaginary frequencies, or, equivalently, a finite Lorentzian width of the delta poles.

3.1 Lanczos dynamics

In the Lanczos formalism the function G_A can be written in the form of a continued fraction:

$$G_A(z) = \frac{\langle \psi_0 | A^\dagger A | \psi_0 \rangle}{z - a_0 - \frac{b_1^2}{z - a_1 - \frac{b_2^2}{z - \dots}}}, \quad (17)$$

where the coefficients a_n and b_n can be obtained using the recursion equation [35]

$$|f_{n+1}\rangle = H|f_n\rangle - a_n|f_n\rangle - b_n^2|f_{n-1}\rangle \quad (18)$$

with

$$|f_0\rangle = A|\psi_0\rangle, \quad a_n = \frac{\langle f_n | H | f_n \rangle}{\langle f_n | f_n \rangle}, \quad b_n^2 = \frac{\langle f_n | f_n \rangle}{\langle f_{n-1} | f_{n-1} \rangle}, \quad \text{and} \quad b_0 = 0. \quad (19)$$

As for finite systems the Green function $G_A(z)$ has a finite number of poles, only a finite number of coefficients (typically less than a few hundreds) a_n and b_n has to be obtained.

For the implementation in the DMRG, one has to take into account several target states using Eq. (2) in order to have a good description of the excitations, for example, the ground state $|\psi_0\rangle$ and the first few $|f_n\rangle$ with $n = 0, 1, \dots$ and $|f_0\rangle = A|\psi_0\rangle$.

3.2 Correction vector dynamics

This method leads to a more precise determination of the spectral functions since it focuses on one particular energy w at a time (or $z = w + i\eta$ if a finite shift is needed). This is achieved by using a correction vector (related to the operator A that can depend on momentum q).

From the Green function Eq. (16), the (complex) correction vector $|x(z)\rangle$ can be defined as

$$|x(z)\rangle = \frac{1}{z - H} A |\psi_0\rangle \quad (20)$$

so the Green function can be calculated as $G(z) = \langle \psi_0 | A^\dagger |x(z)\rangle$. Writing the correction vector in its real and imaginary parts $|x(z)\rangle = |x^r(z)\rangle + i|x^i(z)\rangle$, we obtain

$$\begin{aligned} ((H - w)^2 + \eta^2) |x^i(z)\rangle &= -\eta A |\psi_0\rangle \\ |x^r(z)\rangle &= \frac{1}{\eta} (w - H) |x^i(z)\rangle. \end{aligned} \quad (21)$$

The first equation is solved, for example, using the conjugate gradient method. Here the following target states are kept in the DMRG iterations: the ground state $|\psi_0\rangle$, the first Lanczos vector $A|\psi_0\rangle$ and the correction vector $|x(z)\rangle$. The results lead to reliable excitations for an energy range surrounding this particular point [24].

In [28] a variational formulation of the correction vector technique has been used. From Eq. (21), the following equation is minimized with respect to $|X\rangle$

$$W_{A,\eta}(\omega, X) = \langle X | (H - w)^2 + \eta^2 |X\rangle + \eta \langle \psi_0 | A |X\rangle + \eta \langle X | A | \psi_0\rangle. \quad (22)$$

For any $\eta \neq 0$ and finite ω this function has a well defined minimum for the quantum state which is the solution of Eq. (21), i.e., $|x^i(z)\rangle$.

4 Using the DMRG as the impurity solver for dynamical mean-field theory

Among the most interesting physical phenomena observed in strongly correlated materials, we can mention high-temperature superconductivity, magnetism, ferroelectricity, and the metal-insulator transition. In spite of the enormous efforts devoted to understanding these phenomena, little progress has been achieved, and this is due to the highly complex character involving the strong correlations mainly of localized electrons. These strong correlations are not correctly treated in methods designed for weakly correlated materials such as density-functional theory (DFT) [36] for which the local density approximation (LDA) [37] and other generalizations are used. Thus, non-perturbative numerical methods are the only reliable approach.

To this end, more than twenty years ago, dynamical mean-field theory (DMFT) was developed [38, 39] (see also the chapter by Eva Pavarini). By using it together with LDA it has allowed for band structure calculations of a large variety of correlated materials (see reviews [40, 41]) for which DMFT accounts mainly for local interactions [42, 43].

DMFT consists of a mapping of the correlated system to an effective interacting quantum impurity problem which has to be solved in a self-consistent way. This is the most computationally expensive step within DMFT and determines its success. Since its development, several impurity solvers have been used, like the iterative perturbation theory (IPT) [44, 45], exact diagonalization (ED) [46, 47], the Hirsch-Fye quantum Monte Carlo (HFQMC) [48], the continuous time quantum Monte Carlo (CTQMC) [49–53], non-crossing approximations (NCA) [54],

the numerical renormalization group (NRG) [12, 55–57], the rotationally invariant slave-boson mean-field theory (RISB) [58–60] and quantum chemistry-based techniques [61]. However, they all suffer from limitations, for example, the sign problem and the difficulty in reaching low temperatures in the QMC-based algorithms, the difficulty of the NCA in obtaining a reliable solution for the metallic state, the limitation to few lattice sites of the ED, far from the thermodynamic limit, and the reduced high-energy resolution of the NRG technique.

More recently, to overcome some of these difficulties, an impurity solver based on the DMRG technique was proposed [62–66]. With this method one can obtain the density of states directly on the real frequency axis (or with a very small imaginary offset). This, together with the avoidance of the fermionic sign, is the major advantage given by using the DMRG as compared to QMC impurity solvers. More still, no *a priori* approximations are made and the method provides equally reliable solutions for both gapless and gapped phases. The DMRG impurity-solver provides accurate estimates for the distribution of spectral intensities of high frequency features such as the structure of the Hubbard bands, which is of main relevance for the analysis of x-ray photoemission and optical conductivity experiments, among others.

Subsequent related techniques have been proposed, such as using different methods to obtain the dynamical properties within the DMRG [67, 65], or the time-evolution DMRG algorithm (time evolving block decimation, TEBD) [68] for the one- and two-orbital models [69]. Other developments include the kernel polynomial method (Chebyshev expansion for Green functions) [70, 34, 71], a pole decomposition technique within the correction-vector method for the dynamics [72], the block Lanczos approach [73], the application to non-equilibrium DMFT using MPS [74], and other bath geometries [75]. In this work the authors explore other geometries for the impurity bath, showing an increased efficiency for the star environment. In [76], it was shown that the convergence of the DMFT iterative loops on the imaginary energy axis implies a great reduction of computational costs because, mainly, the imaginary-time evolution does not create entanglement. However, the price to be paid is a reduced resolution on the real-frequency axis.

4.1 Implementation for multi-site and multi-orbital problems

Generalizations of the original DMFT can be considered for these cases, which lead to matrix formulations of the DMFT equations (for details see [66], where the operators are defined within the cell which contains N_c orbitals or sites and which is the effective “impurity” to be solved).

For the general formulation let us consider a Hamiltonian which is the sum of a non-interacting term plus local interactions: $H = H^0 + V$ where $V = \sum_i V_i$ and i is the site or cell index (i.e., the cluster containing N_c sites or orbitals). We define the local operators of H^0 as $h_i^0 = \sum_{IJ} t_{IJ} c_{iI\sigma}^\dagger c_{iJ\sigma}$, where $c_{iI\sigma}^\dagger$ creates an electron in cell i and local “orbital” $I = 1, 2, \dots, N_c$ with spin $\sigma = \uparrow, \downarrow$. We also define the local coefficients $T = (t_{IJ})$.

The main approximation of DMFT is to neglect the self-energy between different cells i and j in the lattice, i.e. to consider only the local self-energy, $\Sigma_{ij}(\omega) \approx \Sigma_{\text{cell}}(\omega) \delta_{ij}$, neglecting spatial correlations to a certain degree, albeit with a good treatment of the local dynamical correlations.

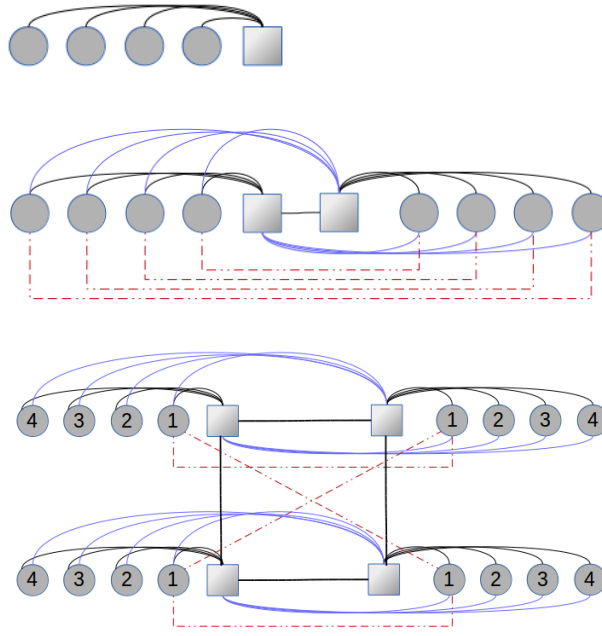


Fig. 2: Schematic representation of Hamiltonian (24) corresponding to the impurity problem for the one, two, and four-site cellular DMFT. See text for details [66].

If we define the non-interacting Green function matrix as $G_0(\omega \mathbf{1} - T)$, the local Green function within the DMFT is now given by [77]

$$G(\omega) = G_0(\omega \mathbf{1} - T - \Sigma(\omega)), \quad (23)$$

which defines the *self-consistency condition* for the $N_c \times N_c$ matrices G and Σ . The lattice problem can now be mapped onto an auxiliary impurity problem that has the same local magnitudes $G(\omega)$ and $\Sigma(\omega)$. This impurity problem should be determined iteratively. Note that G_0 , T , and Σ are $N_c \times N_c$ matrices for the spin-symmetric solution, and $2N_c \times 2N_c$ matrices in the general case. Spatial correlations or the momentum dependence of Σ can be obtained by periodization [78].

The “impurity” Hamiltonian reads

$$H_{\text{imp}} = h_0^0 + V_0 + H_b, \quad (24)$$

where the non-interacting part H_b represents the bath

$$H_b = \sum_{IJq\sigma} \lambda_q^{IJ} b_{Iq\sigma}^\dagger b_{Jq\sigma} + \sum_{IJq} v_q^{IJ} \left[b_{Iq\sigma}^\dagger c_{0J\sigma} + H.c. \right], \quad (25)$$

and $b_{Iq\sigma}^\dagger$ corresponds to the creation operator for the bath-site q , associated to the “orbital” I and spin σ . In Fig. 2 we show a scheme of this effective impurity. Here the circles (squares) represent the non-interacting (interacting impurity) sites. The red lines correspond to the λ_q^{IJ} parameters between bath sites q related to impurities I and J (they are the only hybridization between the baths related to different impurities). The blue lines are the v_q^{IJ} with $I \neq J$ while the black lines are the v_q^{II} . In the bottom scheme we omit some obvious connections for clarity.

The self-consistent iterations of the DMFT can be summarized as follows:

(i) Start with $\Sigma(\omega) = 0$,

(ii) Calculate the Green function

$$G(\omega) = G_0(\omega - T - \Sigma(\omega)), \quad (26)$$

(iii) Obtain the hybridization

$$\Gamma(\omega) = \omega \mathbf{1} - T - \Sigma(\omega) - [G(\omega)]^{-1}, \quad (27)$$

(iv) Find a Hamiltonian representation H_{imp} with hybridization $\tilde{\Gamma}(\omega)$ to approximate $\Gamma(\omega)$. The hybridization $\tilde{\Gamma}(\omega)$ is characterized by the parameters $\mathcal{Y}_q = (v_q^{IJ})$ and $\Lambda_q = (\lambda_q^{IJ})$ of H_b through

$$\tilde{\Gamma}(\omega) = \sum_q \mathcal{Y}_q \cdot [\omega \mathbf{1} - \Lambda_q]^{-1} \cdot \mathcal{Y}_q. \quad (28)$$

(v) Calculate the impurity Green matrix $G_{\text{imp}}(\omega)$ of the Hamiltonian H_{imp} using DMRG,

(vi) Obtain the self-energy

$$\Sigma(\omega) = \omega \mathbf{1} - T - [G_{\text{imp}}(\omega)]^{-1} - \tilde{\Gamma}(\omega). \quad (29)$$

Return to (ii) until convergence.

Step (iv) requires fitting for \mathcal{Y}_q and Λ_q (for details see [66]).

As mentioned above, our problem is completely defined through the parameters V_i , G_0 , and T . Notice that G_0 and T are typically well known one-particle quantities for a given lattice problem. Some particular cases are given below. For example, for the Hubbard model, when considering the single-site, one-orbital DMFT, the defining matrices are $V_i = U n_{i\uparrow} n_{i\downarrow}$, $T = -\mu$ and

$$G_0(\omega - T) = \begin{cases} \frac{1}{N} \sum_{\mathbf{k}} [\omega - \varepsilon(\mathbf{k})]^{-1} & \text{Square lattice} \\ 2 [\omega + \sqrt{\omega^2 - 1}]^{-1} & \text{Bethe lattice} \end{cases}$$

where $\varepsilon(\mathbf{k}) = -2t(\cos k_x + \cos k_y) - 4t' \cos k_x \cos k_y$, with $\mathbf{k} = (k_x, k_y)$ the Fourier space of the square lattice with N sites, $N \rightarrow \infty$, and t (t') the (next-)nearest-neighbor hopping integral [79]. For the 2- or 4-site cluster Hubbard model (called the cellular DMFT [80]), $N_c = 2$ or $N_c = 4$, respectively, and the main matrices are

$$V_i = U \sum_{I=1}^{N_c} n_{iI\uparrow} n_{iI\downarrow}, \quad T = \begin{cases} \begin{pmatrix} -\mu & t \\ t & -\mu \end{pmatrix} & \text{c2-DMFT} \\ \begin{pmatrix} -\mu & t & t & t' \\ t & -\mu & t' & t \\ t & t' & -\mu & t \\ t' & t & t & -\mu \end{pmatrix} & \text{c4-DMFT} \end{cases} \quad \text{and}$$

$$G_0(\omega \mathbf{1} - T) = \frac{N_c}{N} \sum_{\tilde{\mathbf{k}}} \left[\omega \mathbf{1} - \tilde{\varepsilon}(\tilde{\mathbf{k}}) \right]^{-1}.$$

Here, T is the non-interacting intracluster matrix and $\tilde{\varepsilon}(\tilde{\mathbf{k}})$ is the intercluster hopping on the superlattice Fourier space $\tilde{\mathbf{k}}$, which is connected to the one-site lattice through

$$\tilde{\varepsilon}(\tilde{\mathbf{k}})_{IJ} = \frac{1}{N_c} \sum_{\mathbf{K}} \exp \left[i(\mathbf{K} + \tilde{\mathbf{k}}) \cdot \mathbf{R}_{IJ} \right] \varepsilon(\mathbf{K} + \tilde{\mathbf{k}}) \quad (30)$$

with \mathbf{K} the intracluster Fourier-space vectors, see Eq. (23) of [81]. The above implementation is done in a real space clustering, the so-called cellular DMFT (CDMFT). An alternative and complementary cluster approach is the Dynamical Cluster Approximation (DCA). For a detailed analysis between the two see [82].

4.1.1 Example: application to the two-orbital Hubbard model

As an application of this method, we studied the non-hybridized two-orbital Hubbard model with different band widths

$$H = \sum_{\langle ij \rangle \alpha \sigma} t_\alpha c_{i\alpha\sigma}^\dagger c_{j\alpha\sigma} + U \sum_{i\alpha} n_{i\alpha\uparrow} n_{i\alpha\downarrow} + \sum_{i\sigma\sigma'} U_{12} n_{i1\sigma} n_{i2\sigma'}, \quad (31)$$

where $\langle ij \rangle$ are nearest-neighbor sites on a Bethe lattice, $c_{i\alpha\sigma}^\dagger$ creates an electron at site i in orbital $\alpha = 1, 2$ with spin σ , and $n_{i\alpha} = n_{i\alpha\uparrow} + n_{i\alpha\downarrow}$. U (U_{12}) is the intra(inter)-orbital Coulomb repulsion between electrons. The nearest neighbor hoppings are $t_1 \geq t_2$, for bands 1 and 2, respectively. We set $t_1 = 0.5$ which defines the unit of energy and we define $\Delta = U - U_{12}$.

We solved this Hamiltonian at half filling (electron-hole symmetric) using the DMFT with the improved impurity solver based on the DMRG described above, which allowed us to obtain the detailed DOS directly on the real axis directly (or with a very small imaginary offset $0.01 < \eta < 0.2$), zero temperature and system sizes of $L = 40 - 60$ sites. Here we show that, thanks to this combined method, we can observe a rich structure in the DOS which had not been seen before with more approximate techniques. We find that a finite density of states at the Fermi energy in one band is correlated with the emergence of well defined quasiparticle states at excited energies $\Delta = U - U_{12}$ in the other band. We have identified these excitations as inter-band holon-doublon bound states [83] (see Fig. (3)).

In summary, the DMFT+DMRG solver produces reliable results for non-local self energies at arbitrary dopings, hybridizations, and interactions, at any energy scale. It also allows for the calculation of large effective ‘‘impurities’’ to study multi-band interacting models and multi-site or multi-momenta clusters. In addition, it also gives reliable results for the case of real impurity problems, such as adsorbed atoms, cold atoms, and interacting nanoscopic systems like quantum dot arrays among others.

This method paves the way towards the inclusion of additional improvements such as symmetries, finite temperature, and more realistic systems by taking into account configurations given by ab-initio methods.

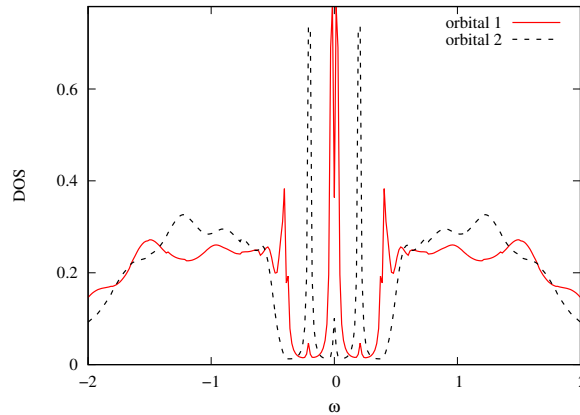


Fig. 3: *Orbital-discriminated DOS for the half-filled two-orbital Hubbard model, (31), for $U = 2.3$, $\Delta = 0.2$ where we observe the existence of in-gap quasiparticle peaks [83].*

5 Conclusions

The DMRG has become one of the most reliable techniques to calculate ground states and dynamical properties of correlated systems. In this lecture we have presented the basic DMRG formalism and given a justification of its performance from a quantum information perspective. This enables the understanding of more recent techniques based on matrix product states and tensor networks. In addition to the calculation of ground state and dynamical properties of models for correlated systems (mainly in low dimensions), we gave an example of how the DMRG can be used to solve the most complex part of the now well established DMFT, i.e, the impurity solver, for the calculation of electronic properties of more realistic models for materials. This technique uses the correction vector to obtain precise Green functions on the real frequency axis directly thus avoiding ill-posed analytic continuation methods from the Matsubara frequencies and fermionic sign problems present in quantum Monte Carlo-based techniques, allowing also for zero temperature calculations. By using a self-consistent bath with low entanglement, it produces precise spectral functions.

Acknowledgements

I would like to acknowledge important contributions of my former PhD student, Yuriel Núñez Fernández, to the optimization of the DMRG as well as to the development and implementation of the DMRG as the impurity solver of the DMFT. I also want to thank my collaborators in this topic, Marcelo Rozenberg, Daniel García, and Pablo Cornaglia for fruitful discussions and joint work. I acknowledge support from projects PICT 2016-0402 from the Argentine ANPCyT and PIP 2015-2017 11220150100538CO (CONICET) and my home institutions, CONICET, CNEA and the University of Cuyo.

References

- [1] S. White, Phys. Rev. Lett. **69**, 2863 (1992)
- [2] S. White, Phys. Rev. B **48**, 10345 (1993)
- [3] I. Peschel, X. Wang, M. Kaulke, and K. Hallberg (eds.): *Density Matrix Renormalization* (Series: Lecture Notes in Physics, Springer, Berlin, 1999)
- [4] K. Hallberg, Adv. Phys. **55**, 477 (2006)
- [5] A. Schollwöck, Rev. Mod. Phys. **77**, 259 (2005); see also R. Noack and S. Manmana, AIP Conf. Proc. **789**, 93 (2005) for a more general review on numerical methods.
- [6] G.K.-L. Chan and S. Sharma, Ann. Rev. Phys. Chem. **62**, 465 (2011)
- [7] S. Wouters and D. van Neck, Eur. Phys. J. D **68**, 272 (2014)
- [8] B. Bauer et al., J. Stat. Mech. P05001 (2011); <http://alps.comp-phys.org>
- [9] <http://quattro.phys.sci.kobe-u.ac.jp/dmrg.html>
- [10] J.C. Bridgeman and C.T. Chubb, J. Phys. A: Math. Theor. **50**, 223001 (2017)
- [11] <http://itensor.org>
- [12] K.G. Wilson, Rev. Mod. Phys. **47**, 773 (1975)
- [13] J. Bray and S. Chui, Phys. Rev. B **19**, 4876 (1979)
- [14] S.R. White and R.M. Noack, Phys. Rev. Lett. **68**, 3487 (1992)
- [15] U. Schollwöck, Ann. Phys. **326**, 96 (2011)
- [16] C. Callan and F. Wilczek, Phys. Lett. B **333**, 55 (1994);
J. Gaiete, Mod. Phys. Lett. A **16**, 1109 (2001)
- [17] J. Latorre, E. Rico and G. Vidal, Quant. Inf. Comp. **6**, 48 (2004)
- [18] G. Vidal, J. Latorre, E. Rico and A. Kitaev, Phys. Rev. Lett. **90**, 227902 (2003)
- [19] V. Korepin, Phys. Rev. Lett. **92**, 96402 (2004)
- [20] In practice it is not necessary to construct the Hamiltonian for the whole system; it is more efficient to handle the blocks separately.
- [21] E. Dagotto, Rev. Mod. Phys. **66**, 763 (1994)
- [22] E.R. Davidson, J. Comput. Phys. **17**, 87 (1975)

- [23] K. Hallberg, Phys. Rev. B **52**, 9827 (1995)
- [24] T. Kühner and S. White, Phys. Rev. B **60**, 335(1999)
- [25] P.E. Dargel, A. Honecker, R. Peters, R.M. Noack, and T. Pruschke, Phys. Rev. B **83**, 161104 (2011)
- [26] P.E. Dargel, A. Wöllert, A. Honecker, I.P. McCulloch, U. Schollwöck, and T. Pruschke, Phys. Rev. B **85**, 205119 (2012)
- [27] S. Ramasesha, Z. Shuai, and J. Brédas, Chem. Phys. Lett. **245**, 224 (1995); S. Ramasesha, S. Pati, H. Krishnamurthy, Z. Shuai, and J.L. Brédas, Phys. Rev. B **54**, 7598 (1996)
- [28] E. Jeckelmann, Phys. Rev. B **66**, 045114 (2002)
- [29] S. White and A. Feiguin, Phys. Rev. Lett. **93**, 076401 (2004)
- [30] U. Schollwöck and S.R. White: *Methods for Time Dependence in DMRG*, in G.G. Batrouni and D. Poilblanc (eds.): *Effective models for low-dimensional strongly correlated systems* (AIP, Melville, New York, 2006)
- [31] J. Sirker and A. Klümper, Phys. Rev. B **71**, 241101 (2005)
- [32] J.J. Garcia-Ripoll, New J. Phys. **8**, 305 (2006)
- [33] A. Holzner, A. Weichselbaum, I.P. McCulloch, U. Schollwöck, and J. von Delft, Phys. Rev. B **83**, 195115 (2011)
- [34] F.A. Wolf, J.A. Justiniano, I.P. McCulloch, and U. Schollwöck, Phys. Rev. B **91**, 115144 (2015)
- [35] E.R. Gagliano and C.A. Balseiro, Phys. Rev. Lett. **59**, 2999 (1987)
- [36] P. Hohenberg and W. Kohn, Phys. Rev. **136**, B864 (1964)
- [37] R.O. Jones and O. Gunnarsson, Rev. Mod. Phys. **61**, 689 (1989)
- [38] G. Kotliar and D. Vollhardt, Physics Today **57**, 53 (2004)
- [39] A. Georges, G. Kotliar, W. Krauth, and M.J. Rozenberg, Rev. Mod. Phys. **68**, 13 (1996)
- [40] M. Imada and T. Miyake, J. Phys. Soc. Jpn. **79**, 112001 (2010)
- [41] K. Held, Adv. Phys. **56**, 829 (2007)
- [42] V.I. Anisimov, A.I. Poteryaev, M.A. Korotin, A.O. Anokhin and G. Kotliar J. Phys.: Condens. Matter **9**, 7359 (1997)
- [43] A.I. Lichtenstein and M.I. Katsnelson, Phys. Rev. B **57**, 6884 (1998)

-
- [44] A. Georges and G. Kotliar, Phys. Rev. B **45**, 6479 (1992)
- [45] M.J. Rozenberg, G. Kotliar, and X.Y. Zhang, Phys. Rev. B **49**, 10181 (1994)
- [46] M. Caffarel and W. Krauth, Phys. Rev. Lett. **72**, 1545 (1994)
- [47] Y. Lu, M. Höppner, O. Gunnarsson and M.W. Haverkort, Phys. Rev. B **90**, 085102 (2014)
- [48] J.E. Hirsch and R.M. Fye, Phys. Rev. Lett. **56**, 2521 (1986)
- [49] A.N. Rubtsov, V.V. Savkin, and A.I. Lichtenstein, Phys. Rev. Lett. **72**, 035122 (2005)
- [50] P. Werner, A. Comanac, L. de Medici, M. Troyer, and A.J. Millis, Phys. Rev. Lett. **97**, 076405 (2006)
- [51] H. Park, K. Haule, and G. Kotliar, Phys. Rev. Lett. **101**, 186403 (2008)
- [52] E. Gull, A.J. Millis, A.I. Lichtenstein, A.N. Rubtsov, M. Troyer, and P. Werner, Rev. Mod. Phys. **83**, 349 (2011);
E. Gull, P. Werner, O. Parcollet, and M. Troyer, EPL **82**, 57003 (2008)
- [53] Y. Nomura, S. Sakai, and R. Arita, Phys. Rev. B, **91**, 235107 (2015)
- [54] T. Pruschke, D.L. Cox, and M. Jarrell, Phys. Rev. Lett. **47**, 3553 (1993)
- [55] R. Bulla, Phys. Rev. Lett. **83**, 136 (1999);
R. Bulla, A.C. Hewson, and T. Pruschke, J. Phys.: Cond. Mat. **10**, 8365 (1998)
- [56] K.M. Stadler, Z.P. Yin, J. von Delft, G. Kotliar, and A. Weichselbaum, Phys. Rev. Lett. **115**, 136401 (2015)
- [57] K.M. Stadler, A.K. Mitchell, J. von Delft, and A. Weichselbaum, Phys. Rev. B **93**, 235101 (2016)
- [58] F. Lechermann, A. Georges, G. Kotliar, and O. Parcollet, Phys. Rev. B **76**, 155102 (2007)
- [59] A. Isidori and M. Capone, Phys. Rev. B **80**, 115120 (2009)
- [60] M. Ferrero, P.S. Cornaglia, L. De Leo, O. Parcollet, G. Kotliar, A. Georges, EPL **85**, 57009 (2009)
- [61] D. Zgid and G.K.-L. Chan, J. Chem. Phys. **134**, 094115 (2011);
D. Zgid, E. Gull, and G.K.-L. Chan, Phys. Rev. B **86**, 165128 (2012)
- [62] D.J. García, K. Hallberg, and M.J. Rozenberg, Phys. Rev. Lett. **93**, 246403 (2004)
- [63] D.J. García, E. Miranda, K. Hallberg, M.J. Rozenberg, Phys. Rev. B **75**, 121102(R) (2007)
- [64] Y. Núñez Fernández, D. García, and K. Hallberg, J. Phys.: Conf. Series **568**, 042009 (2014); Y. Núñez Fernández and K. Hallberg, Papers in Physics **9**, 090005 (2017)

- [65] M. Karski, C. Raas, and G. Uhrig, *Phys. Rev. B* **72**, 113110 (2005)
- [66] Y. Núñez Fernández and K. Hallberg, *Front. Phys.* **6**, 13 (2018)
- [67] S. Nishimoto, F. Gebhard, and E. Jeckelmann, *J. Phys.: Condens. Matter* **16**, 7063 (2004)
- [68] G. Vidal, *Phys. Rev. Lett.* **93**, 040502 (2004); G. Vidal, *Phys. Rev. Lett.* **91**, 147902 (2003)
- [69] M. Ganahl, M. Aichhorn, P. Thunström, K. Held, H.G. Evertz, and F. Verstraete, *Phys. Rev. B* **92**, 155132 (2015)
- [70] A. Weisse, G. Wellein, A. Alvermann and H. Fehske, *Rev. Mod. Phys.* **78**, 275 (2006)
- [71] M. Ganahl, P. Thunström, F. Verstraete, K. Held, and H.G. Evertz, *Phys. Rev. B* **90**, 045144 (2014)
- [72] R. Peters, *Phys. Rev. B* **84**, 075139 (2011)
- [73] T. Shirakawa and S. Yunoki, *Phys. Rev. B* **90**, 195109 (2014)
- [74] F. Wolf, I. McCulloch and U. Schollwöck, *Phys. Rev. B* **90**, 235131 (2014)
- [75] D. Bauernfeind, M. Zingl, R. Triebl, M. Aichhorn, and H.G. Everts, *Phys. Rev. X* **7**, 031013 (2017)
- [76] F.A. Wolf, A. Go, I.P. McCulloch, A.J. Millis, U. Schollwöck, *Phys. Rev. X* **5**, 041032 (2015)
- [77] E. Pavarini, E. Koch, D. Vollhardt, and A. Lichtenstein (eds.): *DMFT at 25: Infinite Dimensions* (Forschungszentrum Jülich, 2014)
<http://www.cond-mat.de/events/correl14>
- [78] T. Stanescu and G. Kotliar, *Phys. Rev. B* **74**, 125110 (2006)
- [79] S. Sakai, Y. Motome, and M. Imada, *Phys. Rev. B* **82**, 134505 (2010)
- [80] G. Kotliar, S. Savrasov, G. Pálsson, and G. Biroli, *Phys. Rev. Lett.* **87**, 186401 (2001)
- [81] T. Maier, M. Jarrell, T. Pruschke, and M. Hettler, *Rev. Mod. Phys.* **77**, 1027 (2005)
- [82] E. Koch, G. Sangiovanni, and O. Gunnarsson, *Phys. Rev. B* **78**, 115102 (2008)
- [83] Y. Núñez Fernández, G. Kotliar, and K. Hallberg, *Phys. Rev. B* **97**, 121113(R) (2018)